International Journal for Housing Science and Its Applications
Publish August 3, 2025. Volume 46, Issue 3 Pages 44-60

https://doi.org/10.70517/ijhsa46304

Digital Extraction of Traditional Patterns Based on Wavelet Transform and Modern Design Application in the Perspective of Cultural Inheritance

Wenxin Lei[1], Jiyang Gao[1,*], Shanshan He[2] and Xiaohui Ming[1]
[1] Qilu University of Technology (Shandong Academy of Sciences), Jinan, Shandong, 250353, China
[2] Beijing Institute of Technology, Beijing, 100081, China
Corresponding authors: (e-mail: lwenxin789@163.com).

Abstract In order to protect and inherit the excellent traditional culture and enhance the economic value of cultural industry, the article proposes a method of digital extraction and modern design application of traditional patterns based on digital means to adapt to the development of today's society and the transformation of consumer demand. The article first combines the traditional pattern pattern with the characteristics of texture directionality, and proposes an adaptive weighted feature fusion traditional pattern feature extraction algorithm that introduces wavelet energy analysis. Subsequently, a traditional pattern style classification algorithm based on capsule network is proposed to improve the traditional pattern classification accuracy. Then a traditional pattern style migration method based on VGG19 network is designed, which is applied to modern design, and the performance test and subjective and objective evaluation of this paper's method are conducted. The experimental results show that the method of this paper can realize the modern design of traditional patterns with good effect, and compared with the classical slow style migration and fast style migration methods, it has better image conversion quality and higher conversion efficiency, which can provide a certain design and development of reference value for modern pattern design.

Index Terms wavelet transform, capsule network, VGG19 network, style migration, traditional pattern

I. Introduction

China's five thousand years of civilization has a long history and deep heritage, which has given birth to China's rich traditional culture, which contains the deepest spiritual connotation of the Chinese nation, manifests the unique spiritual imprint of the Chinese nation, and has a high research value [1]-[3]. As a crucial part of Chinese cultural resources, traditional culture plays an irreplaceable role in the inheritance and development of Chinese civilization. Nowadays, the total number of intangible cultural heritage in China is close to 870,000 items, of which only 1,557 national-level resources exist, and more than half of the items are at risk of being lost [4]. In most of the intangible cultural projects rich in traditional pattern elements, the patterns show partial or comprehensive blurring, missing, deformation and other phenomena due to factors such as temporal and spatial changes, environmental impacts, human interference, etc., and the risk of loss of heritage increases due to the complexity of production techniques in the process of inheritance [5]-[8]. Protecting and passing on traditional patterns is an important area of cultural inheritance today.

In recent years, China has continuously raised the importance of the development of traditional cultural inheritance and elevated the inheritance of excellent traditional culture to a new level, i.e., digital protection and inheritance. With the rapid development of computer technology and digitization technology, the preservation and development of traditional patterns have been constantly innovated [9]. At present, preserving and modernizing the application in digital form is an important means of inheriting traditional culture and improving the public's understanding of traditional culture. In the context of the new era, the use of modern technical means and methods to achieve the innovative development of traditional culture, from a single material preservation to the development of non-material application and dissemination, to achieve the sustainability of traditional culture [10]-[13]. Accompanied by the call to make cultural heritage manifest the vitality of the new era and the protection and application of traditional patterns, the use of digital technology to promote the integration of traditional culture and science and technology with the support of modern technology has been a general trend [14], [15].

With the increasing development of economic globalization, the use of traditional patterns has become increasingly popular and popular. Under the strong support of national policies, the national tide culture has emerged

and ushered in a golden period of development. The national tide culture integrates traditional culture and the spirit of the times, takes the national brand as the carrier, the excellent quality as the connotation, and the modern technology as the means to satisfy the consumers' demands for fashion and cultural self-confidence, and it has the profound significance of diversified fusion and cross-border innovation [16], [17]. Patterns, as an indispensable element in national trend design, have a strong visual presentation effect and are also an important form of externalization of traditional cultural connotations [18]. Traditional patterns can be seen everywhere in history, and are widely present on decorations such as clothing, carpets, architecture, porcelain, etc., as well as appearing in large numbers on sculptures, murals, paintings and calligraphy, and other works of art. As a symbol of traditional Chinese culture, rich patterns have rich and diversified pattern types and combination shapes, which not only reflect the superior craftsmanship and artistic aesthetics of the predecessors, but also fully reflect the natural, introverted and harmonious cultural connotation of the Chinese nation, which is favored by modern designers [19]-[22]. Mainly presented in the clothing, cultural creation, beauty, handmade, games, packaging, furniture, construction and other on products. For example, Yu-Ming et al. [23] not only optimized the creative quality of the product, but also satisfied the consumer's demand experience by extracting the characteristics of the “Nine Quarters of Flowering River” pattern of the Chinese Miao people and applying it to the design of modern canvas bags through innovative design. Fan [24] improved the design based on the traditional tiger stripe pattern and embedded the pattern into men's clothing design, which not only inherited the traditional pattern, but also enriched the content of men's clothing design. Li et al [25] categorized traditional auspicious motifs (textual and graphical) and designed a 3D model in which the innovative design of auspicious motifs was carried out to complete the sustainability of traditional auspicious motifs. Jiang [26] mentions that taotie motifs and bronzes are widely used in furniture such as tableware in modern restaurants, but also in other spatial environments within the store, creating a dining environment rich in traditional culture. Hou [27] describes the application of traditional Chinese patterns to the external packaging design of products in a trendy environment, which attracts consumers' eyes and improves the added value of the products at the same time. It can be seen that the application of traditional patterns in modern design is an important direction to improve the added value of modern products. However, in the current application of traditional patterns, there is often pattern distortion, resulting in pattern inheritance deviation, which is due to the application of patterns floating on the surface, without in-depth observation of pattern details.

In both the digital inheritance and application of traditional patterns, it is necessary to digitally extract the patterns in order to obtain information about their pattern characteristics, so as to carry out tasks such as pattern restoration, patching, and innovation. Han et al [28] learned and trained four convolutional neural network models for automatic extraction of patterns on ceramics, and this extraction method is not only advantageous in terms of speed, but also allows for batch pattern extraction. Liang [29] utilized a multilevel histogram algorithm to segment the traditional patterns so as to realize the extraction of pattern features. Compared with HOD (Histograms of Oriented Gradients), GIF (Graphics Interchange Format) algorithm, RSDF (Random Split and Deep Forest) algorithms, the multilevel histogram algorithm has better performance. Shi et al [30] constructed a framework for ancient textile pattern contour extraction using the human visual system with the help of computer vision technology and proved the effectiveness of the framework. Cai et al [31] used an improved recurrent generative adversarial network to extract lines from images of traditional dress patterns and contour images, and classified the images, combined three loss functions, and outputted the extraction to achieve fine traditional pattern line extraction. However, the applicability of these methods is low due to the complexity of the process and the varying degrees of damage to the extracted target patterns. Also, the study lacks cultural semantic extraction of traditional patterns.

The wavelet transform (WT), on the other hand, gradually carries out multi-scale refinement of the signal (function) through telescopic translation operations, and eventually achieves time subdivision at high frequencies and frequency subdivision at low frequencies, which can automatically adapt to the requirements of time-frequency signal analysis, and thus can be focused to any details of the signal [32]. Divakar et al [33] proposed an image edge detection pattern recognition method supported by discrete WT, which focuses on image recognition by decomposing the image at different levels and performing edge analysis and description of the target image through difference image, reconstructed image, and edge detection. Laimeche et al [34] introduced a Zipf curve image feature extraction method containing a WT that incorporates Zipf's law, which is superior to the histogram feature extraction method, and it has a very good localization property in both time and frequency domains, which better solves the contradiction between the resolution of the time and frequency domains.

The article firstly proposes an adaptive feature fusion algorithm for traditional pattern feature extraction by combining the characteristics of traditional pattern texture directionality, obtaining the texture band reconstruction image by wavelet decomposition and extracting the improved LBP features by uniform chunking, and introducing the energy analysis to compute the feature weights for weighted fusion to form the fused feature DWT-LBP. Subsequently, based on the capsule network, the SE module is introduced in the convolutional layer by to pay

attention to the channel information of traditional patterns, so as to improve the performance of the whole network model for traditional pattern style classification. Then, based on the network structure and style migration principle of VGG19 network, the migration number, weight ratio, pooling method and objective optimization algorithm that are more suitable for traditional pattern migration are explored. In the performance testing part, the feasibility of capsule network in texture image classification application and the ability of classification performance improvement are investigated, and the robustness of the algorithm is analyzed through anti-rotation and anti-noise experiments. Finally, subjective and objective evaluations of modern pattern designs after applying the methods of this paper are conducted.

II. Traditional pattern feature extraction based on adaptive feature fusion

II. A. Wavelet transform and local binary modes

II. A. 1) Wavelet transform theory

Wavelet transform (WT) has the property of multi-scale and multi-resolution analysis, and the wavelet transform is classified into two types: continuous wavelet transform (CWT) and discrete wavelet transform (DWT). Where the classification is based on whether the parameters of the wavelet are discretized or not. Assuming that a wavelet basis $\phi(t)$ is given, there are:

$$\phi_{a,b}(t)=\frac{1}{\sqrt{a}}\phi\left(\frac{t-b}{a}\right) \tag{1}$$

where $\phi_{a,b}(t)$ is a family of functions, a is the stretching transform (scale) factor and b is the displacement transform factor [35]. Common continuous wavelet basis functions include: dbN wavelet basis, Sym wavelet basis, $Haar$ wavelet basis, $bior$ wavelet basis, $Coif$ wavelet basis, and so on.

For any signal $f(t)$, if it satisfies $f(t)\in L^2(R)$, i.e., the signal has finite energy, the continuous wavelet transform is defined as follows:

$$\begin{aligned} CWT_f(a,b)&=\frac{1}{\sqrt{a}}\int_{-\infty}^{+\infty}f(t)\phi\left(\frac{t-b}{a}\right)dt \\ &=\int_{-\infty}^{+\infty}f(t)\phi_{a,b}(t)dt \end{aligned} \tag{2}$$

where t is a continuous random variable and $a>0$. As the parameter a increases, the time width of the $\phi\left(\frac{t}{a}\right)$ analysis of the signal $f(t)$ increases and vice versa. The displacement factor b determines the initial position at which the signal $f(t)$ is analyzed.

The discrete wavelet transform (DWT) is a raster sampling of the CWT parameters: scale factor a and displacement factor b. DWT greatly reduces the computational complexity and facilitates computer processing.

(1) Scale factor discretization: the scale factor a is power-scaled so that $a=a_0^m, m\in Z$, $m\in Z$, then the corresponding wavelet function is $a_0^{\frac{-j}{2}}\phi\left[a_0^{-j}(t-b)\right]$, $j=0,1,2,\cdots$.

(2) Discretization of the displacement factor: in order to be able to cover the entire time axis, a uniform discrete value is usually taken for b. Then $\phi_{a,b}(t)$ is:

$$\begin{aligned} \phi_{a,b}(t)&=a_0^{\frac{-j}{2}}\phi\left[a_0^{-j}\left(t-ka_0^jb_0\right)\right] \\ &=a_0^{\frac{-j}{2}}\phi\left(a_0^{-j}t-kb_0\right) \end{aligned} \tag{3}$$

Then the discrete wavelet transform is defined as:

$$DWT_f\left(a_0^j,kb_0\right)=\int_{-\infty}^{+\infty}\phi_{a_0,kb_0}(t)f(t)dt \tag{4}$$

II. A. 2) Local binary mode

The LBP algorithm takes the local region of the image as a processing unit, the threshold is set as the gray value of the center point of the local unit, and then the grayscale of the neighboring pixel points in the local unit is sequentially compared with the threshold value. When the grayscale value of the neighboring point is greater than or equal to the threshold value, it is coded as 1, and if it is less than it is coded as 0. Finally, the thresholded sequence of numbers (0 or 1) is converted to a decimal number that is the LBP value of the center pixel point.The formula of the LBP operator is shown below:

$$LBP = \sum_i s(g_i - g_c) * 2^i \tag{5}$$

where $s(x) = \begin{cases} 1, g_i \geq g_c \\ 0, Other \end{cases}$, g_i denotes the gray value of the neighboring pixel point, and g_c denotes the gray value of the neighboring center pixel point.

In order to further improve the ability of the LBP operator to describe the image, for the original LBP can not capture the image large-scale texture structure, to enhance the robustness to the image rotation changes and to solve the problem of the feature dimension is too high, et al. proposed a rotation-invariant LBP mode, uniform LBP mode, defined as in Eqs. (6), (7).

$$LBP_{r,p}^{ri} = \min\left\{ROR\left(LBP_{r,p}, i\right), i = 0,1,\cdots,p-1\right\} \tag{6}$$

Where p and r represent the number of pixel points in the neighborhood and the radius of the neighborhood, respectively. $ROR(x,i)$ is the rotation function by which the encoded binary sequence is cyclically shifted and the LBP value is computed, with the minimum value being the final LBP value.

$$\begin{aligned} U\left(LBP_{(P,R)}\right) &= \left|s\left(g_{p-1} - g_c\right) - s\left(g_0 - g_c\right)\right| \\ &+ \sum_{p=1}^{P-1}\left|s\left(g_p - g_c\right) - s\left(g_{p-1} - g_c\right)\right| \end{aligned} \tag{7}$$

where $U\left(LBP_{(P,R)}\right)$ is the metric factor of the uniform mode, which indicates the number of 0/1 (or 1/0) transformations in the encoded binary sequence. A uniform LBP pattern is defined when $U\left(LBP_{(P,R)}\right)$ does not exceed 2.

II. B.Fusion feature extraction based on adaptive weighting

In this section, we use DWT to combine the characteristics of directional description with the directionality of traditional pattern texture, extract the improved LBP features by uniformly chunking the reconstructed images of the low-frequency proximity subbands, horizontal, vertical, and diagonal high-frequency subbands of the DWT decomposition, and calculate the percentage of the energy distribution of the four subbands in order to determine the fusion weight of the features, and the fusion features by adaptive weighting are used to accurately classify, and the DWT-LBP feature extraction is shown in Fig. 1. The DWT-LBP feature extraction process is shown in Figure 1.

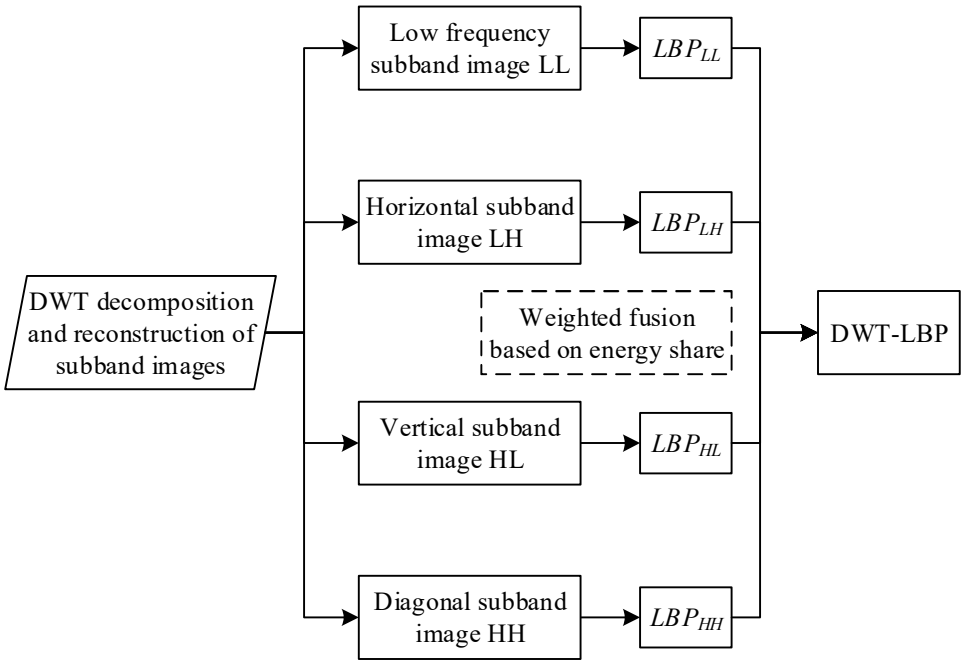

Figure 1: DWT-LBP feature extraction process

II. B. 1) Reconstructed image acquisition after DWT decomposition

According to the texture directionality characteristics of traditional pattern patterns, the authors classify the traditional pattern pattern images into four types: horizontally oriented, vertically oriented, diagonally oriented, and irregular.DWT has the advantage of multi-scale analysis, and the image can be decomposed by DWT to obtain the low-frequency approximation subbands, and the three high-frequency detail subbands, horizontally, vertically, and diagonally. The authors propose to perform one layer of DWT decomposition on the original tire tread image and use four subband wavelet coefficients for image reconstruction to obtain the low-frequency approximation subband image LL, the horizontal high-frequency detail image LH, the vertical high-frequency detail image HL, and the diagonal high-frequency detail image HH.

II. B. 2) Chunking to extract improved LBP features

The LBP operator can portray valuable essential information in an image, and is an excellent descriptor with high discriminative power, low computational complexity, and resistance to illumination interference and rotational changes. To enhance the robustness of the LBP model to noise, we propose to uniformly chunk the reconstructed pattern images of four subbands with $5*5$ size. Since the size of pixel gray values in similar regions of the image is similar, in order to overcome the change of the center pixel value due to noise, the average local gray (ALG) of the neighborhood of each sub-block is used as a threshold to compute the LBP coding instead of the value of its center pixel.The ALG is defined as follows:

$$ALG = \frac{\sum_x \sum_y g_{xy} + g_c}{25} \tag{8}$$

where g_c denotes the center pixel value of the sub-block and g_{xy} represents the gray value of the pixels in the neighborhood of the sub-block.

II. B. 3) Fusion feature weight assignment strategy

Feature extraction of the four subbands reconstructing the conventional pattern yields rotationally invariant homogeneous LBP features for the pattern's low-frequency approximation subbands, and for the three high-frequency detail subbands, horizontally, vertically, and diagonally, which are denoted as LBP_{LL}, LBP_{LH}, LBP_{HL}, LBP_{HH}. The features of the four subband reconstructed images describe the feature information of different directions of the pattern. We propose a weighted fusion of the four features. The four subbands after DWT one-layer decomposition have different ability to describe the information of the pattern and the amount of energy they occupy. We introduce an energy analysis method to determine the weights of the features by calculating the energy sizes of the four subbands, and propose a feature fusion method based on adaptive weighting of the energy share. Among them, the low-frequency approximation subband image LL is the best approximation of the original pattern image. Therefore, weighted fusion is performed by calculating the percentage of each subband energy to the sum of the four subband energies as the weight of that subband feature as shown in the following equation.

$$E_k = \sum_i \sum_j C_{ij}^2 \tag{9}$$

$$E_{sum} = E_{LL} + E_{LH} + E_{HL} + E_{HH} \tag{10}$$

$$\alpha_k = \frac{E_k}{E_{sum}} \tag{11}$$

where $k = LL, LH, HL, HH$, C_{ij} denotes the wavelet coefficients of each pixel of each sub-band in the frequency domain by DWT decomposition, E_k denotes the energy of sub-band k, E_{sum} is the sum of the energy of the four sub-bands, and α_k is each sub-band's energy percentage i.e., the feature weights. This produces a normalized weighted fusion feature:

$$F_{fise} = \left\{ \alpha_{LL} \cdot LBP_{LL}, \alpha_{LH} \cdot LBP_{LH}, \alpha_{HL} \cdot LBP_{HL}, \alpha_{HH} \cdot LBP_{HH} \right\} \tag{12}$$

III. Traditional pattern style classification based on improved capsule network

In order to enhance the extraction of traditional pattern features and thus improve the accuracy of traditional pattern style classification, this section explores and proposes an algorithm for traditional pattern style classification based on capsule networks.

III. A. Capsule Networks

A layer of neurons in the hidden layer of a neural network is called a “capsule”. A capsule is a new architecture for neural networks. A capsule is a packaged set of neurons, which is equivalent to a normal neural network in some

parts, but the difference is that the neurons output numerical values, while the capsule outputs vectors, the length of which indicates the extent to which the capsule recognizes the features, and carries a certain amount of gesture information, and the direction of which indicates the attributes of the entity.

III. A. 1) Capsule network structure

The network structure of the capsule network is schematically shown in Fig. 2, with an image size input of 28 × 28 × 1. It mainly includes a convolutional layer, which is used to extract the feature information in the image or feature map. The main capsule layer is used to vectorize the feature information to obtain the feature vector. Digital capsule layer, which is used to convert feature vectors to high-dimensional feature vectors through dynamic routing [36]. Fully connected layer for classifying the high dimensional feature vectors.

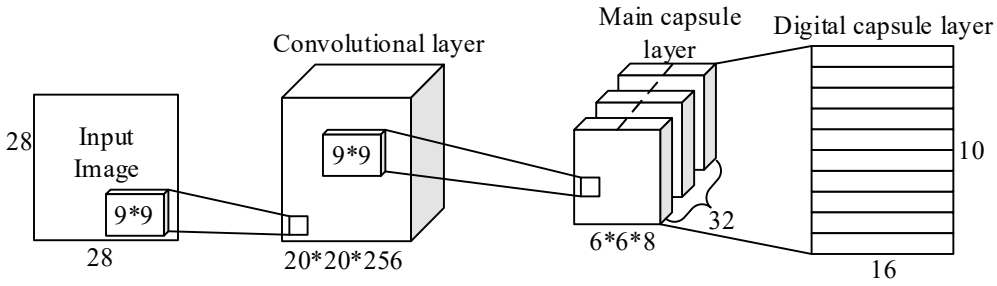

Figure 2: Network structure of capsule network

The architecture of the capsule network reconstruction network is shown in Fig. 3, containing 512, 1024, and 784 neurons, respectively, and the final structure of the output is adjusted to a size of 28 × 28 for the calculation of the reconstruction loss.

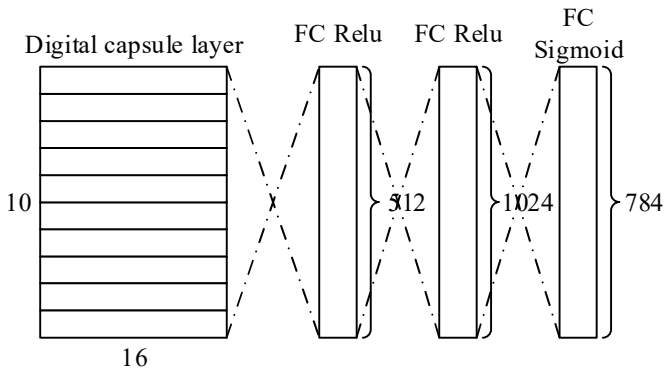

Figure 3: Architecture of the capsule network reconstruction network

III. A. 2) Capsule network loss function

The capsule network uses an edge loss function as the final loss of the network, which consists of a cost loss and a reconstruction loss and can be expressed as shown in Equation (13):

$$L_c = T_c \max\left(0, m^+ - \|v_c\|\right)^2 + \lambda\left(1 - T_c\right)\max\left(0, \|v_c\| - m^-\right)^2 \tag{13}$$

where c is some kind of categorized category, T_c is the indicator of the categorization, which determines whether the predicted category exists or not (1 means the existence of the class of c, 0 means the nonexistence of the class of c), and m^+, and m^- are generally set to 0.9, 0.1, which are used for controlling the predicted probability of the category of the output to make the probability is greater than 0.9. $\|v_c\|$ denotes the probability that the predicted category truly belongs to this category.

When the predicted class c does not exist and T_c is 0, the first part of Eq. When the predicted class c exists and the second part of Eq. is 0, $\|v_c\|$ will not be less than 0.9, and if the class c does not exist, $\|v_c\|$ will not be greater than 0.1, and the $0.1, \lambda$ coefficient is generally taken as 0.5, in order to reduce the loss generated by the nonexistent class, so that the stability of the formula data can be ensured.

III. A. 3) Capsule Network Routing Rules

The "prediction vector" $\hat{u}_{j|i}$ in the capsule network is represented by Eq. (14) as follows:

$$\hat{u}_{j|i} = W_{ij} u_i \tag{14}$$

where W_{ij} is the transform weight matrix for dynamic routing, i is the vector index of the lower capsule layer L, j denotes the vector index of the higher capsule layer $L+1$ corresponding to the vector i, and u_i denotes the instantiation parameter of the lower capsule i, and the transform matrix W_{ij} encodes the spatial features, which contain the relative relationships between the low-level, and high-level features, and is updated by back-propagation through the training process.

Then, the intermediate result $\hat{s}_j$ is obtained by weighted summation of high-level features $\hat{u}_{j|i}$ by Eq. for dynamic routing of features:

$$\hat{s}_j = \sum_i c_{ij} \hat{u}_{j|i} \tag{15}$$

Where the parameter c_{ij} is the coupling coefficient between the L layer capsule i and the $L+1$ layer capsule j, which indicates the probability of routing the L layer capsule i to the $L+1$ capsule j layer, which is updated iteratively through dynamic routing, and the higher value of this value indicates that it is more important.

Normalized by SoftMax function, the calculation formula is represented by equation (16):

$$c_{ij} = \frac{\exp\left(b_{ij}\right)}{\sum_j \exp\left(b_{ij}\right)} \tag{16}$$

Where: each initialized coupling coefficient is the same, and SoftMax can make the parameters c_{ij} all positive and sum to 1.

b_{ij} is the a priori probability that the capsule i is connected to the capsule j, which is continuously updated according to the iterative update of the dynamic routing, and initialized to 0. The process is shown in Equation (17):

$$b_{ij} \leftarrow b_{ij} + \hat{u}_{j1i} \cdot v_j \tag{17}$$

At the first iteration, b_{ij} is initialized to 0 and $0, \hat{u}_{j1i} \cdot v_j$ represents the inner product of the vectors, which increases as the angle of the vector pinch decreases, and vice versa, when the angle of the vectors increases, the inner product results in a decrease.

After the output of the main capsule layer has been dynamically routed, in order to ensure that the length is between 0 and 1, it is necessary to use a nonlinear activation function to compress the value of the length between (0, 1) and to make the capsule in the same direction to achieve this goal. The realization process is shown in Equation (18):

$$v_j = \frac{\left\|s_j\right\|^2}{1+\left\|s_j\right\|^2} \frac{s_j}{\left\|s_j\right\|} \tag{18}$$

III. B. Channel Attention Mechanisms

SE network module whose input feature maps X are of equal importance for each channel. After a series of convolution operations or pooling operations (transformation F_{tr}), the U feature map is obtained. Then the feature map U is squeezed by channel dimension to fuse the $\mathrm{H}\times\mathrm{W}$ features in the feature map, and weights are added to each channel after the squeezing operation so as to recalibrate each channel in the feature map U [37].The SE module consists of the following three main operations.

Compression operation: the features are compressed using spatial dimensions, and the 2D features of each channel are compressed to a real number by global average pooling, which is implemented as shown in the following expression of Eq. (19):

$$Z_c = F_{sq}\left(u_c\right) = \frac{1}{w * H} \sum_{i=1}^{w} \sum_{j=1}^{H} u_c(i, j) \tag{19}$$

Where $W \times H$ is a 2D feature and u is a tensor feature weight.

Stimulus operation: generate weight values by predicting the importance of all the channels, and then act these weight values on the channels corresponding to the previous feature map, which is realized as shown in Eq. (20).

$$s_c = F_{ex}\left(z, w\right) = \sigma\left(g(z, w)\right) = \sigma\left(W_2 \delta\left(W_1 z\right)\right) \tag{20}$$

Where σ is the activation function Sigmoid function and δ is the activation function ReLU function.

Feature recalibration operation: multiply the channel weights obtained from the excitation operation by the input features to realize the recalibration of the feature map, which is realized as shown in Equation (21).

$$\tilde{x}_c = F_{scale}(u_c, s_c) = s_c * u_c \tag{21}$$

III. C. Improved capsule network model incorporating SEs

III. C. 1) Feature Enhancement Extraction Module

In this paper, we introduce a module based on an attention mechanism that learns the importance of different channels, and then weights the features on each channel according to the importance of the channels learned by the SE module of the channel attention mechanism, so as to highlight the important features, while selectively suppressing the feature channels that are not useful for the current classification task, thus enhancing the feature expression ability of the model. Robust features are extracted in the model of the feature enhancement module by overlaying deeper network structures and attention mechanisms. For the feature maps extracted from the primary features, the channel attention mechanism is employed, which is utilized to give more attention to the valuable features and suppress the feature channels that are not useful for pattern style classification to ignore irrelevant information.

The feature enhancement operation can be defined as equation (22):

$$\begin{aligned} F_t &= F_{t-1} \cdot \sigma\left(W_2 \delta\left(W_1\left(\frac{1}{H \times W}\sum_{i=1}^{H}\sum_{j=1}^{W} F_{t-1}(i,j)\right)\right)\right) \\ F_{t+1} &= W_3^{1\times 3}\left(W_3^{3\times 1}\left(M_2\left(F_t\right)\right)\right) \end{aligned} \tag{22}$$

where H is the height of the feature map, W is the width of the feature map, W is the convolution operation, σ and δ represent different activation functions, and M is the maximum pooling operation.

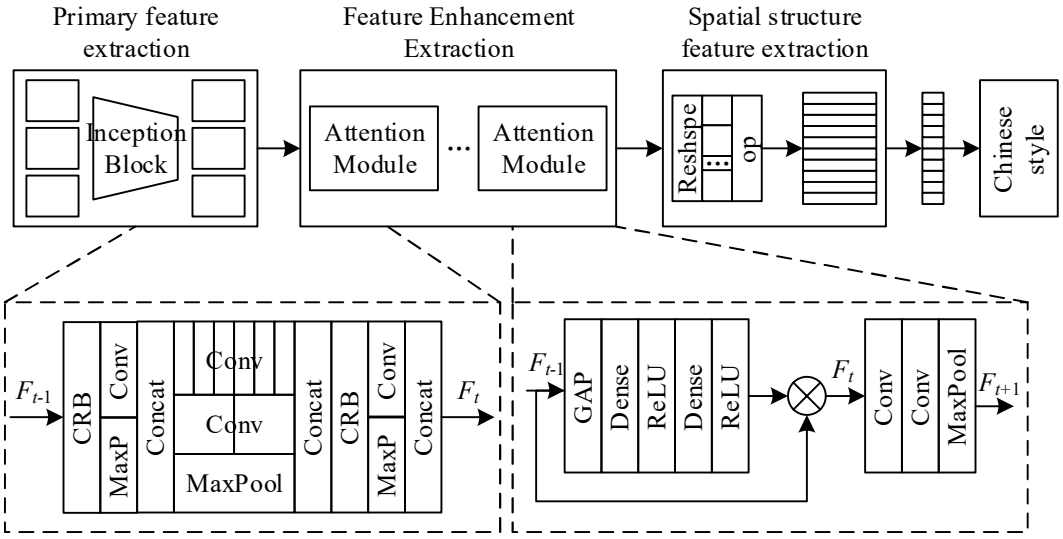

Figure 4: Structure diagram of capsule network based on feature enhancement

III. C. 2) Improved Capsule Network Integral Model for Fusion of SEs

The structure of the capsule network based on feature enhancement is shown in Fig. 4. The network model has a total of three modules: the first module is the primary feature extraction network module, the second module is the feature enhancement extraction network module, and the third module is the capsule network module. By inputting the pattern into the first module, downsampling and feature extraction are performed on the input image, and then the extracted feature map is passed into the second module, and the channel attention mechanism is applied to pay attention to the content information in its channel, and the feature information is gradually weighted and optimized, and finally the obtained feature map is inputted into the capsule network structure to enhance the spatial features and classify the features, so as to improve the network model to improve the classification of features while maintaining the rate. The network model can improve the classification performance while maintaining the rate.

IV. Traditional pattern style migration based on VGG19 network

IV. A. Network structure of VGG19

The VGG19 network structure mainly consists of 5 convolutional blocks, 3 fully connected layers, and each convolutional block contains a convolutional layer, a ReLU layer, and a pooling layer, for a total of 19 parameter layers. The network uses all 3×3 convolutional kernels.

IV. B. Principles of style migration in the VGG19 network

The VGGNet model consists of two parts: a convolutional layer and a fully connected layer. The convolutional layer extracts image features, and the fully connected layer is equivalent to the probability of converting the extracted "features" in the image into categories.The VGG16 and VGG19 models can extract more image features as the structural level of the VGGNet model gets deeper. Style Migration reconstructs the original image from the input features.

In the Content Reconstructions process, we use is to reconstruct the image method is the gradient descent method, define a content loss $L_{content}(\vec{p},\vec{x})$, the content loss is used as the optimization objective of the gradient descent method, and the formula for the content loss of a certain layer is defined as follows:

$$L_{content}(\vec{p},\vec{x},l)=\frac{1}{2}\sum_{i,j}\left(F_{ij}^{l}-P_{ij}^{l}\right)^{2} \tag{23}$$

The $\vec{p}$ in the formula represents the original image of the input, and $\vec{x}$ represents the final reconstruction to get the image. The l represents the number of levels of convolutional layers, i represents the channel position of convolution, and j represents the j th convolutional position. P_{ij}^{l} represents the convolutional features of the input original image $\vec{p}$ at the l th layer, the i th channel, and the j th position. The F_{ij}^{l} represents the convolution feature at $\vec{x}$ at the l th layer, i th channel, and j th position. Convolutional features can usually be expressed in terms of height, width, and number of channels. The j usually denotes the height and width. Assuming that the convolution feature is $50\times50\times64$, the correspondences therein, $1\leq i\leq 64$, $1\leq j\leq 2500$. From the formula it can be seen that $L_{content}(\vec{p},\vec{x},l)$ is the L_2 distance at which the convolutional features are computed, i.e., this distance represents the difference between the content of the original image of the input and the content of the image that is obtained from the final reconstruction. If this value is larger, it means that the original image and the reconstructed image are more different in content, and if this value is smaller, it means that the original image and the reconstructed image are more similar in content. After the input of the original image, a reconstructed image $\vec{x}$ is randomly initialized, and according to the definition of content loss, the optimization direction is to minimize the content loss $L_{content}(\vec{p},\vec{x})$, and after iteration, $\vec{x}$ will constantly converge to the final image that wants to be reconstructed The

For Style Reconstructions. The style of an image is quantized by the Gram matrix of the features of the convolutional layer. The Gram matrix is a special kind of metric matrix. It is usually formed by the inner product of two vectors in Euclidean space with respect to each other. It is a symmetric matrix. The form is as follows:

$$\begin{bmatrix}\left(\overrightarrow{X_1},\overrightarrow{X_1}\right) & \left(\overrightarrow{X_1},\overrightarrow{X_2}\right) & \cdots & \left(\overrightarrow{X_1},\overrightarrow{X_n}\right)\\ \left(\overrightarrow{X_2},\overrightarrow{X_1}\right) & \left(\overrightarrow{X_2},\overrightarrow{X_2}\right) & \cdots & \left(\overrightarrow{X_2},\overrightarrow{X_n}\right)\\ \cdots & \cdots & \cdots & \cdots\\ \left(\overrightarrow{X_n},\overrightarrow{X_1}\right) & \left(\overrightarrow{X_n},\overrightarrow{X_2}\right) & \cdots & \left(\overrightarrow{X_n},\overrightarrow{X_n}\right)\end{bmatrix} \tag{24}$$

The Gram matrix-based style migration method uses the Gram matrix to measure the stylistic differences between images, a statistic that can be computed. Let G_{ij}^{l} be the j th element in row 1 of the Gram matrix. F_{ij}^{l} is the output of the l th convolutional layer, then the convolutional feature can be expressed as follows:

$$G_{ij}^{l}=\sum_{k}F_{ik}^{l}F_{jk}^{l} \tag{25}$$

Suppose a certain layer l, the height of the convolutional features, the size of the width is M_l and the number of channels is N_l. Then F_{ij}^{l} satisfies the conditions $1\leq i\leq N_l$, $1\leq j\leq M_l$. The Gram matrix G vector set is $F_1^l,F_2^l,\cdots F_i^l,\cdots,F_{N_l}^l$. And $F_{N_l}^{l}=\left(F_{i1}^{l},F_{i2}^{l},\cdots,F_{ij}^{l},\cdots,F_{iM_l}^{l}\right)$. In the l layer, F_1^l represents the first channel feature and F_2^l represents the 2nd channel feature, and they are vectors of the same dimension.

With the Gram matrix as a quantization criterion, the style of the image can also be mimicked by content reconstruction by formulating a style loss L_{style} and reconstructing the image style using the style loss. The style loss $L_{style}(\vec{a},\vec{x},l)$ formula for a certain layer is as follows:

$$L_{style}(\vec{a},\vec{x},l)=\frac{1}{4N_l^2M_l^2}\sum_{ij}\left(G_{ij}^l-A_{ij}^l\right)^2 \tag{26}$$

Where $\vec{a}$ represents the input stylized image and $\vec{x}$ represents the image to be reconstructed. The input image $\vec{a}$ has a Gram matrix A^l obtained after convolutional processing in the l th layer, and the image to be reconstructed $\vec{x}$ has a Gram matrix G^l obtained after convolutional processing in the l th layer. Considering that the order of magnitude of content loss and style loss can cause large errors if the difference is too large, and certain features may be enlarged or reduced, a normalization term $4N_l^2M_l^2$ is added in the formula to map the values of the style loss to a certain range. In image style migration, the style loss $L_{style}(\vec{a},\vec{x},l)$ derived from the convolution of a particular layer is often insufficient, and it is common to compute multiple layers of style loss and then sum them according to a certain weight to get the total style loss $L_{style}(\vec{a},\vec{x})$. The total image style loss expression is:

$$L_{style}(\vec{a},\vec{x})=\sum_{i=0}^{l}w_lL_{style}(\vec{a},\vec{x},l) \tag{27}$$

Where $\vec{a}$ represents the input stylized image and $\vec{x}$ represents the image to be reconstructed. The w_l represents the weight occupied by the l th layer. The image content and style are split apart with a content loss $L_{content}(\vec{p},\vec{x})$ to reconstruct the image content, a style loss $L_{style}(\vec{a},\vec{x})$ to reconstruct the image style, and then re-combined according to the weights to generate the new image. Define a total image loss function $L_{total}(\vec{p},\vec{a},\vec{x})$ with the expression:

$$L_{total}(\vec{p},\vec{a},\vec{x})=\alpha L_{content}(\vec{p},\vec{x})+\beta L_{style}(\vec{a},\vec{x}) \tag{28}$$

In this equation, $\vec{p}$ represents the content image, $\vec{a}$, represents the style image, and $\vec{x}$ represents the final generated image. The final generated image can have both the content of the content image $\vec{p}$ and reflect the style of the style image $\vec{p}$. The two hyperparameters α, β in Eq. are used to harmonize the image content and style. With a large parameter α, the generated image $\vec{x}$ possesses a little bit more distinctive features of $\vec{p}$ content, and with a large parameter β, the generated image $\vec{x}$ will be more close to the style of $\vec{a}$.

V. Algorithmic performance testing

V. A. Experimental environment

The experiments were conducted on three commonly used texture image datasets, namely KTH-TIPS-2b (KTH), Kylberg Texture Dataset v.1.0 (KTD), and UIUC Texture Dataset (UIUC).The KTH dataset was obtained by expanding the KTH-TIPS dataset to include more challenging color The KTH dataset is an extension of the KTH-TIPS dataset and contains more challenging color texture images, with 11 categories of texture image samples acquired at 9 distance scales, 4 viewing angles and 3 light intensities, each containing 4 physical entities. The KTD dataset contains two datasets, with and without rotation, and the no-rotation dataset has a total of 20 categories of texture images, each of which is acquired from the same object under the same acquisition conditions for 4 consecutive acquisitions. The UIUC dataset contains 25 texture categories, and each image is randomly acquired under conditions with significant view angle changes and from different physical entities.The training and test sets of the three datasets are divided as shown in Table 1.

Table 1: Different data sets

Data set	KTH	KTD	UIUC
Train set	3622	3252	721
Test set	1175	1325	306
Class	13	20	25
Type	Color	Gray	Gray
Total number of images	4763	4495	1000

V. B. Classification performance test of wavelet capsule network for texture images

For classification testing of texture images for wavelet capsule network, the texture image is first used as input to the wavelet capsule network after scaling the size of the texture image to 128pixel×128pixel. Then data augmentation is performed on the input image using data augmentation technique, which consists of data augmentation operations such as flipping the image horizontally, vertically and randomly rotating it by 15° to prevent overfitting. Finally, iterative training of 100 epochs is performed. The initial learning rate of the model is set to 0.002, and the learning rate is adjusted to half of the original one for every 10 epochs of iterative training. The classification accuracies of the wavelet capsule network trained and tested on three commonly used texture image datasets are shown in Fig. 5 (Fig. a is the training set and Fig. b is the test set). It can be seen that the wavelet capsule network converges faster and there is no overfitting or underfitting.

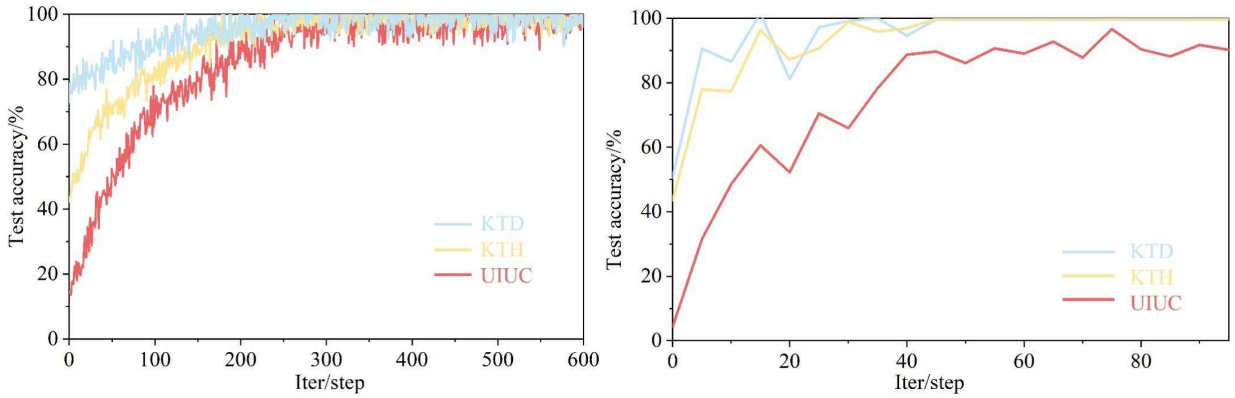

(a) Training set (b) Test set

Figure 5: Classification accuracy

The classification accuracy of different texture classification algorithms on KTH, KTD and UIUC datasets is shown in Table 2. From the table, it can be found that the classification accuracy of wavelet capsule network is higher compared to local binary pattern (LBP), elevated local binary pattern (ILBP) and fuzzy local binary pattern (FLBP) algorithms, and the classification accuracy of the wavelet capsule network is higher when compared to the GPBMFD, local quantization coding (LQC), sorted local gradient pattern (SLGP), local concave-convex microstructural pattern (LCCMSP), and local quaternion pattern (LQPAT) algorithms can improve the classification accuracy by a maximum of 17.13 percentage points on the KTH dataset and 8.89 percentage points on the KTD dataset compared to the LQPAT algorithm. This indicates that the wavelet capsule network can realize the automatic extraction of features and learn a richer representation of texture features than the manually designed features, so as to better describe the texture features and achieve better classification results.CNN-based texture such as T-CNN-3, Visual Classification Network (VisualNet), VGG-VD-16, Deep-Texture Encoding Network (Deep-TEN) and LFV image classification algorithms utilize the powerful feature representation capability of CNNs with better classification performance. The wavelet capsule network combines the multi-resolution analysis ability of wavelet transform and the expression ability of DCNN, which can simultaneously learn the interrelationships between features, further improving the texture feature expression ability of the algorithms and obtaining better texture classification results. Compared with the CNN-based texture image classification algorithm, the wavelet capsule network achieves better classification results on different texture image datasets. The highest classification accuracy was achieved on both KTH and KTD datasets, 99.96% and 99.32%, respectively. On the UIUC dataset, the classification accuracy of the wavelet capsule network is 92.33%. This proves that wavelet capsule networks have excellent texture representation performance and are very effective in traditional pattern classification tasks.

In order to verify the data differentiation ability of the wavelet capsule network, the output features of the wavelet capsule network on the KTD training set are visualized using the t-distributed random neighbor embedding algorithm using the KTD dataset as an example, and the visualization of the output features of the DTWCapsNet is shown in Fig. 6. Where all color points are colored according to the real labels. It can be found that the output features of wavelet capsules are characterized by compact intraclass aggregation and clear interclass distance, which indicates that the output features of wavelet capsule networks have good discriminative power and are conducive to classification recognition.

Table 2: Classification accuracy of different texture classification algorithms

Type	Model	KTH/%	KTD/%	UIUC/%
Traditional algorithm	LBP	90.07	97.76	89.32
	ILBP	96.44	91.35	91.46
	FLBP	93.84	90.43	89.29
	GPBMFD	--	--	91.38
	LQC	96.32	--	92.78
	SLGP	95.25	--	--
	LCCMSP	94.21	92.22	--
	LQPAT	82.83	97.67	--
CNN-based algorithm	T-CNN-3	99.66	73.44	--
	VisualNet	72.19	99.16	--
	VGG-VD-16	99.85	99.03	92.31
	Deep-TEN	85.05	--	--
	LFV	81.95	--	--
Ours		99.96	99.32	92.33

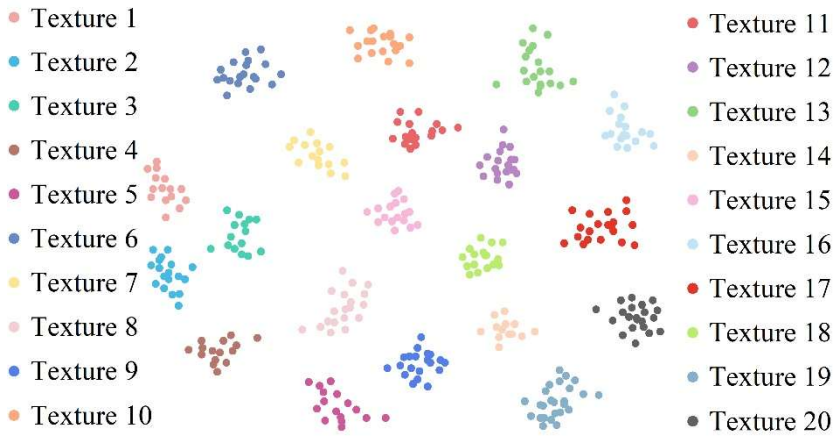

Figure 6: Visual effect

The dataset used for the experiment contains both color and grayscale images, in order to study the effect of color and grayscale images on the classification performance of wavelet capsule network, the sample images in the KTH dataset are first grayscale processed, and then experimented as the input to the DTWCapsNet, and the classification accuracies on both color and grayscale texture images are shown in Table 3. Where KTH-color denotes the original color sample image and KTH-gray denotes the grayscale processed KTH sample image. It can be found that the difference between the classification effectiveness of the wavelet capsule network on color texture images and grayscale texture images is small. The reason is that color texture images provide richer color features, and the wavelet capsule network can effectively utilize the color information provided by color images to obtain higher classification accuracy.

Table 3: Classification accuracy on color and grayscale texture images (%)

Data set	KTH-color	KTH-gray
Accuracy	99.65	96.32

V. C. Noise immunity test of wavelet capsule network

Wavelet capsule networks have demonstrated strong learning and representation capabilities on three commonly used texture image datasets, but texture images acquired in natural scenes usually contain a large amount of noise, which has a great impact on the correct classification of texture images, so the noise-resistant capability of the model is particularly important in the texture image classification task.

Keeping the structural division of the original dataset of KTH unchanged, Gaussian noise $N(0,\sigma^2)$ is added to all sample images as new data samples for model training and testing to simulate noisy texture images collected under natural conditions. Noise with variance σ^2 as an indicator of noise level was added in order σ^2 =0.01, 0.03, 0.05, 0.07, 0.09 for the experiments. The sample images containing different noises are trained for 100 iterations to obtain the classification accuracy of the test set of KTH dataset with different noise levels, and the classification accuracy of the wavelet capsule network on different noise levels (KTH dataset) is shown in Fig. 7. It can be found that the classification accuracy of the wavelet capsule network decreases after adding noise, but with the increasing noise level, the effect of noise on the classification accuracy of the wavelet capsule network is within the acceptable range, which indicates that the wavelet capsule network has good noise robustness.

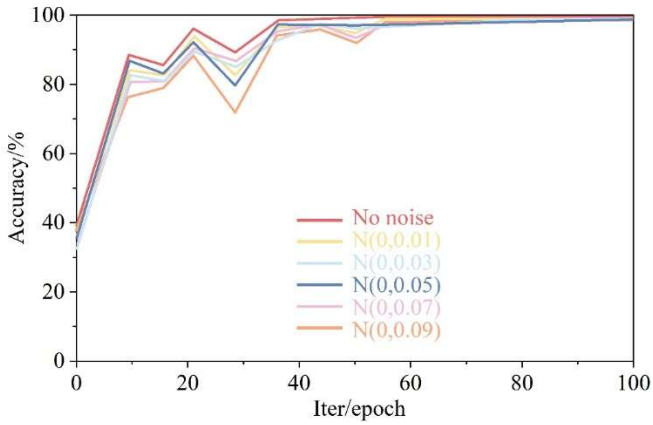

Figure 7: The classification accuracy of wavelet capsule network in different noise levels

V. D. Anti-rotation performance test of wavelet capsule network

The excellent performance of wavelet capsule networks on texture image classification tasks cannot be separated from the diversity of data samples. When the sample diversity is insufficient, the model learns relatively fewer features, thus affecting the classification performance. Rotation transformation is also a factor that affects sample diversity, in order to test the anti-rotation performance of wavelet capsule networks, experiments are carried out with KTD with rotated dataset.The rotated data of KTD has 12 kinds of rotational angles, and the images rotated by 0° are randomly divided into the training set and the test set according to the ratio of 3:1, and then 50 traditional patterns are randomly sampled as the test set from the images of each class with different angles, and the wavelet capsule The network training process does not introduce any rotational transformation, and the classification accuracy of the wavelet capsule network on the rotated image dataset is shown in Table 4. It can be found that the wavelet capsule has some anti-rotation robustness and has a large room for improvement.

Table 4: The classification accuracy of wavelet capsule network

Rotation angle/(°)	Accuracy/%
0	99.76
30	67.25
60	44.75
90	51.47
120	41.48
150	57.11
180	96.26
210	64.33
240	41.53
270	50.81
300	43
330	62.14

V. E. Style Migration Experiment

The dataset used for the experiments in this section contains two parts: the traditional pattern dataset and the modern pattern dataset. A total of 500 rounds were trained, and the changes of the loss function during the training process are shown in Fig. 8. The pre-trained model with 200 rounds was chosen for testing because the loss decrease decreased or even difficult to continue decreasing after 200 rounds of training.

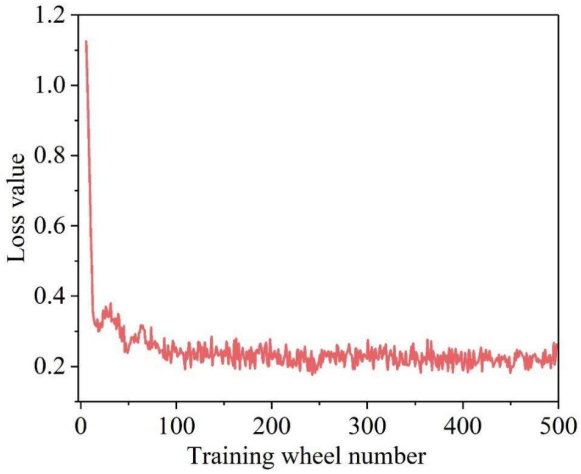

Figure 8: Changes in the loss function during the training process

VI. Effects of modern design applications of traditional motifs

VI. A. Objective evaluation analysis

An objective evaluation analysis with peak signal-to-noise ratio PSNR and structural similarity SSIM, and a comparison of multiple commonly used normalization techniques is shown in Figure 9 (Figures a and b show the experiments on the PSNR and SSIM datasets, respectively). As can be seen from the figure, the PSNR value of the method used in this paper is lower than the slow style migration method (Gatys) but higher than the fast style migration method (Johnson). The image SSIM value of this paper's method is then higher than the other 2 classical methods. Therefore, the style transformation quality of this paper's method is good and the structural features are better preserved.

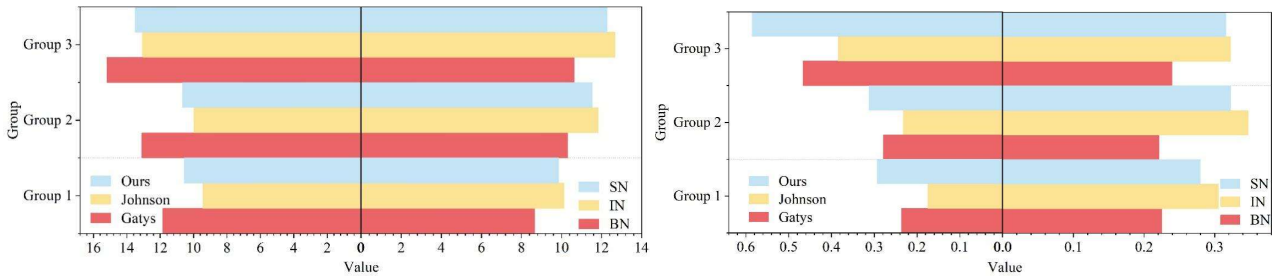

(a) PSNR (b) SSIM

Figure 9: A variety of common normalized techniques

This section evaluates the conversion efficiency of the algorithm in terms of whether the algorithm needs to be trained, whether it supports conversion of arbitrary styles, and the speed of conversion. The algorithm evaluation is shown in Table 5. The style migration method in this paper has the ability to handle a large number of stylization tasks by training only one stylization model and the conversion speed is three orders of magnitude faster compared to the slow style migration method (Gatys). And compared to the fast style migration method (Johnson), there is only a slight decrease in the efficiency of the training and conversion process, but the image conversion quality is higher. The self-adaptive normalization technique SN and the instance normalization technique IN are close to each other in terms of style conversion quality, and both are higher than the batch normalization BN used for the original conversion network, but spend relatively less time on training.

Table 5: Algorithm evaluation

Algorithm	Training time/min	Any style	Conversion speed		
			256×256	512×512	1024×1024
Gatys	0	Yes	>1h	>1h	>1h
Johnson	109	Training	0.755s	2.001s	6.856s
Ours	122	Training	1.032s	3.185s	11.263s

VI. B. Subjective evaluation

A certain number of pictures were first viewed by the test subjects and subsequently scored on the evaluation scale of the graphic scheme. After statistical analysis of the scoring data from the recovered questionnaires, the evaluation results of the test subjects were obtained. The evaluation of the results of the modern pattern generated based on the method of this paper is shown in Table 6. A total of 28 people thought that the pattern completely continued or basically continued the traditional pattern style (mean score 1.22). A total of 25 people thought that the pattern fully conformed or basically conformed to contemporary aesthetics (mean score of 0.68). The average scores of both results are greater than 0. The evaluation data indicate that the modern pattern design using the method of this paper not only continues the artistic style of the traditional pattern, but also caters to the aesthetic orientation of contemporary people.

Table 6: Based on the modern pattern results of this method

Question	Attitude	Number	Score	Average score
Does it continue the style of traditional patterns	No traditional pattern (-2)	0	1	1.22
	Not too handy for traditional patterns (-1)	2	4	
	General (0)	2	3	
	It's basically a traditional pattern (1)	16	14	
	It's a complete continuation of the traditional pattern (2)	12	10	
Whether it meets contemporary aesthetic needs	Completely not in the same time as the aesthetic (-2)	1	-2	0.68
	Not very contemporary (-1)	2	-4	
	General (0)	4	0	
	Basic in contemporary aesthetics (1)	16	12	
	Perfect in contemporary aesthetics (2)	9	17	

VII. Conclusion

The article explores the modernized design application method of traditional patterns under the perspective of cultural inheritance, and the research results can provide certain reference value for modern pattern design.

In the classification accuracy experiments of different texture classification algorithms, the classification accuracy of this paper's algorithm on the KTH and KTD datasets can be maximally improved by 17.13 and 8.89 percentage points, which indicates that DWT-LBP can realize the automatic extraction of features, and wavelet capsule network has a good effect of traditional pattern classification.

In the subjective evaluation experiments, 25 people think that the patterns generated by using the method of this paper are fully in line with contemporary aesthetics. The modern pattern design using the method of this paper not only continues the artistic style of traditional patterns, but also caters to the aesthetic orientation of contemporary people.

Funding

Shandong Province Social Science Planning Research Project in 2021, “Research on the Presentation Methods of Visual Arts in the Context of Digital Media”, Item No. 21CWYJ12.

About the Author

Jiyang Gao, Professor, Vice Dean, Master's Degree Supervisor of College of Art and Design, Qilu University of Technology (Shandong Academy of Sciences), Postdoctoral Fellow of Shandong University, Visiting Scholar of the University of London, Director of Design Education Committee of China Society of Higher Education, Member of Shandong Province Professional Degree Postgraduate Education Steering Committee, Vice Chairman of Jinan Young Artists' Association, Vice Chairman of Jinan Cultural and Creative Design Society, Expert of Shandong Province Department of Industry and Informatisation. Vice Chairman of Jinan Young Artists Association, Vice

Chairman of Jinan Cultural and Creative Design Society, Expert of Shandong Industrial and Information Technology Department.

Academy of Sciences) in 2023. She is currently pursuing her master's degree in the College of Art and Design, Qilu University of Technology (Shandong Academy of Sciences). Her research interests include visual communication design, and design history.

Shanshan He, Associate Professor, Master's Degree Supervisor, Head of Visual Communication Department, School of Art and Design, Qilu University of Technology.She has published three books, namely “Composition and Design”, “Color Composition” etc. She has also published over ten papers (works) including “Research on the Dissemination Path of Red Culture in the Context of New Media”, “Preventing Environmental Pollution”, “Book Appreciation”, etc. I have presided over five provincial and ministerial-level projects such as “Research on the Aesthetic of Ming and Qing Dynasty Woodblock Books” and “Research on the Presentation Methods of Visual Arts in the Context of Digital Media”, as well as three projects at the departmental and bureau level.

Xiaochuan Ming received the B.S. degree in automation from Ocean university of China in 2023. He is currently pursuing the M.S. degree with the School of Automation, Beijing Institute of Technology, Beijing, China. His research interests include pneumatic detection and control, model identification and control.

References

[1] Liu, J., Krotova, T. F., Yezhova, O., & Pashkevich, K. (2018). Traditional elements of Chinese culture in logo design. International Circular of Graphic Education and Research.

[2] Xuan, W. (2022). On the Significance and Methods of Inheriting and Developing Chinese Traditional Culture. Academic Journal of Humanities & Social Sciences, 5(11), 46-50.

[3] Yang, Y. (2023). The Triple Dimension of Excellent Chinese Traditional Culture and Its Contemporary Value. International Journal of Social Science and Humanity, 13(1).

[4] Dang, Q., Luo, Z., Ouyang, C., Wang, L., & Xie, M. (2021). Intangible cultural heritage in China: a visual analysis of research hotspots, frontiers, and trends using citeSpace. Sustainability, 13(17), 9865.

[5] Zhang, Y. (2024). The Evolution and Contemporary Expression of Traditional Chinese Patterns: Water Patterns and Cloud Patterns as Examples. Mediterranean Archaeology and Archaeometry, 24(1), 112-122.

[6] Xiao, P., & Legino, R. (2022). Problems and Countermeasures in the Inheritance of Chinese Traditional Culture: the example of Chinese traditional patterns. Environment-Behaviour Proceedings Journal, 7(SI9), 485-489.

[7] Xu, Q. (2023). The Intangible Heritage of Mogao Grottoes Mural Characteristics: Educational Role of Pattern Art and Its Impact on Art Education. Mediterranean Archaeology and Archaeometry, 23(3), 171-184.

[8] Chen, L., Mohamad, W. S. A. B. W., & Arif, M. F. B. M. (2024). EXAMINING CHINESE HAINAN MIAO ETHNIC PATTERNS: EMBRACING NATURE’S INFLUENCE THROUGH ECOLOGICAL THEMES, SHAPES, AND COLORS IN DESIGN. Arts Educa, 41.

[9] Xi, C., & Chung, J. (2024). Research on the Use of AI for Digitalization and Dissemination of Traditional Chinese Art Patterns. International Journal of Advanced Culture Technology, 12(4), 231-236.

[10] Peters, N., Marinova, D., van Faassen, M., & Stasiuk, G. (2017). Digital preservation of cultural heritage. Technology, Society and Sustainability: Selected Concepts, Issues and Cases, 107-114.

[11] Li, Z. (2022). Exploring the Path of Innovative Development of Traditional Culture under Big Data. Computational Intelligence and Neuroscience, 2022(1), 7715851.

[12] Chen, H., & Zheng, X. (2021, February). Application of traditional culture based on computer technology in modern visual communication design. In Journal of Physics: Conference Series (Vol. 1744, No. 3, p. 032094). IOP Publishing.

[13] Chen, Z. (2024). An Analysis of the Impact of Digital Media on the Sustainable Development of Traditional Culture Conducted. Advances in Economics, Management and Political Sciences, 84, 237-241.

[14] Cahyaningrum, Y., Kinanthi, S., Magfiroh, A. I., & Ramdhani, D. E. (2024, December). Blending Cultural Heritage with Digital Design: A New Era in Pottery Motifs and Art. In Proceeding of the International Conference on Mathematical Sciences, Natural Sciences, and Computing (Vol. 1, No. 2, pp. 88-99).

[15] Gondoputranto, O., & Dibia, I. W. (2022). The use of technology in capturing various traditional motifs and ornaments: A case study of batik fractal, Indonesia and TUDITA-Turkish digital textile archive. Humaniora, 13(1), 39-48.

[16] Lin, G., Hao, L., & Yong, W. (2022). A Study on the Value of Cultural Self-confidence Cultivated by the Rise of" National Tide. Academic Journal of Humanities & Social Sciences, 5(5), 29-34.

[17] Zhang, Y. (2022, February). The Application and Practice of Traditional Cultural Symbols in the Brand Design of “Nation Tide”. In 2021 conference on art and design: Inheritance and innovation (ADII 2021) (pp. 266-270). Atlantis Press.

[18] Qiudao, L. (2023). Analysis on the Application Method of Weifang Traditional Kite Schema in Cultural Creative Products. Frontiers in Art Research, 5(4).

[19] Han, D., & Cong, L. (2023). Miao traditional patterns: the origins and design transformation. Visual Studies, 38(3-4), 425-432.

[20] Zhang, J., & Yang, X. (2023). Exploring the Archaeological Treasures of the Silk Road: Tibetan Arts and Crafts, Traditional Decorative Patterns, and Pattern Symbols Analysis. Mediterranean Archaeology and Archaeometry, 23(2), 197-212.

[21] Xu, B. (2021). The inheritance and creative design of traditional color scheme based on modern consumer's psychological perception: Taking Chinese traditional decorative pattern's color collocation as an example. Color Research & Application, 46(4), 856-870.

[22] Pan, Y., Luo, Q., & Xu, Z. (2024). The diversified influence of Ming and Qing porcelain symbols on modern clothing patterns and cultural and artistic connotations from the perspective of intangible cultural heritage. Mediterranean Archaeology and Archaeometry, 24(3), 148-162.

[23] Yu-Ming, M., He-min, D., & Hao, Y. (2023). On innovative design of traditional Chinese patterns based on aesthetic experience to product features space mapping. Cogent Arts & Humanities, 10(2), 2286732.

[24] Fan, J. (2023). The Application of Chinese Traditional Tiger Pattern in Men's Fashion Design. International Journal of Advanced Culture Technology, 11(1), 253-262.
[25] Li, D., Park, J., Kim, S. H., & Liu, S. (2022). Developing sustainable clothing design using Chinese auspicious patterns. International Journal of Costume and Fashion, 22(2), 14-28.
[26] Jiang, Y. (2023). Application of Traditional Chinese Patterns in Modern Restaurant Space Design. Journal of Building Technology, 5(2), 2717-5103.
[27] Hou, M. (2025). The Application of Traditional Chinese Patterns in National Tide Packaging Design. Curriculum Learning and Exploration, 2(4).
[28] Han, L., Wang, Y., & Wang, X. (2023, October). Typical ceramic pattern extraction based on convolutional neural network. In 2023 International Conference on Culture-Oriented Science and Technology (CoST) (pp. 42-46). IEEE.
[29] Liang, X. (2022). Traditional Pattern Feature Extraction and Cultural Creative Design Application Based on Multilevel Histogram Shape Segmentation. Mobile Information Systems, 2022(1), 3581570.
[30] Shi, X., Xu, Z., Cui, L., Zhao, X., & Zhang, W. (2024). ViCo: Human visual perception-based contour extraction of Chinese Tang dynasty textile patterns. Textile Research Journal, 00405175241268771.
[31] Cai, X., Jia, S., Yao, J., Wu, Y., & Sun, H. (2023, August). An Image Extraction Method for Traditional Dress Pattern Line Drawings Based on Improved CycleGAN. In Computer Graphics International Conference (pp. 312-323). Cham: Springer Nature Switzerland.
[32] Yang, G., Dai, J., Liu, X., Chen, M., & Wu, X. (2020). Spectral feature extraction based on continuous wavelet transform and image segmentation for peak detection. Analytical methods, 12(2), 169-178.
[33] Divakar, R., Singh, B., Bajpai, A., & Kumar, A. (2022). Image pattern recognition by edge detection using discrete wavelet transforms. Journal of Decision Analytics and Intelligent Computing, 2(1), 26-35.
[34] Laimeche, L., Merouani, H. F., & Mazouzi, S. (2018). A new feature extraction scheme in wavelet transform for stego image classification. Evolving Systems, 9, 181-194.
[35] Amar Kumar Verma,Prerna Saurabh,Deep Madhukant Shah,Vamsi Inturi,Radhika Sudha,Sabareesh Geetha Rajasekharan & Rajkumar Soundrapandiyan. (2024). A wavelet and local binary pattern-based feature descriptor for the detection of chronic infection through thoracic X-ray images.. Proceedings of the Institution of Mechanical Engineers. Part H, Journal of engineering in medicine,238(11-12),9544119241293007.
[36] Huiyun Zhang,Heming Huang,Puyang Zhao & Zhenbao Yu. (2025). Sparse temporal aware capsule network for robust speech emotion recognition. Engineering Applications of Artificial Intelligence,144,110060-110060.
[37] Shang Yunhao,Xu Ning,Jin Zhenzhou & Yao Xiao. (2022). Optimization of the routing of capsule network based on multiscale information and self-attention mechanism.(eds.)Hohai University,IoT Engineering,Changzhou,China.